

Nonreciprocal recovery of electromagnetically induced transparency by wavenumber mismatch in hot atoms

Lida Zhang (张理达)¹, Nina Stiesdal², Hannes Busche², Mikkel Gaard Hansen², Thomas Pohl³, and Sebastian Hofferberth²

¹School of Physics, East China University of Science and Technology, Shanghai, 200237, China

²Institut für Angewandte Physik, University of Bonn, Wegelerstr. 8, 53115 Bonn, Germany

³Institute for Theoretical Physics, Vienna University of Technology (TU Wien), 1040 Vienna, Austria

Abstract. For multi-level systems in hot atomic vapors the interplay between the Doppler shift due to atom velocity and the wavenumber mismatch between driving laser fields strongly influences transmission and absorption properties of the atomic medium. In a three-level atomic ladder-system, Doppler broadening limits the visibility of electromagnetically-induced transparency (EIT) when the probe and control fields are co-propagating, while EIT is recovered under the opposite condition of counter-propagating geometry and $k_p < k_c$, with k_p and k_c being the wavenumbers of the probe and control fields, respectively. This effect has been studied and experimentally demonstrated as an efficient mechanism to realize non-reciprocal probe light transmission, opening promising avenues for example for realization of magnetic-field free optical isolators. In this tutorial we discuss the theoretical derivation of this effect and show the underlying mechanism to be an avoided crossing of the states dressed by the coupling laser as a function of atomic velocities when $k_p < k_c$. We investigate how the non-reciprocity scales with wavelength mismatch and show how to experimentally demonstrate the effect in a simple Rydberg-EIT system using thermal Rubidium atoms.

1. Introduction

The phenomenon of electromagnetically induced transparency (EIT) has emerged as a key technique for quantum optics since the first observations three decades ago [1–8], allowing for example coherent photon storage and memory in atomic media [9–14]. Introducing long-lived Rydberg-states into EIT ladder-schemes [15] enables novel applications such as electric and magnetic field sensing [16–22] and few-photon nonlinearities [23–26]. The latter have been used for single-photon sources [27–30], photon-atom entanglement [31], single-photon switches [32–34], photon subtraction [35, 36] and photonic quantum gates [37–39].

In hot atomic vapors, atomic motion and the resulting Doppler shift strongly influences the EIT effect [15, 40–46]. More specifically, the observed transmission depends on the projection of the vector sum of the probe and control wavevectors \mathbf{k}_p and \mathbf{k}_c onto the probe beam direction. Interestingly, this makes three-level EIT systems inherently non-reciprocal in the sense that reversing the probe beam direction along the same propagation axis, while keeping the control field fixed, can result in completely different transmission [47, 48].

For typical atomic lambda-systems with probe and control fields of approximately equal wavelength ($k_p = |\mathbf{k}_p| \approx k_c = |\mathbf{k}_c|$) the Doppler effect is mitigated by a co-propagating beam geometry [49, 50]. However, the residual Doppler broadening due to the small wavenumber mismatch between the two fields leads to both a narrowing of the EIT window and nonvanishing absorption inside the window [51]. In contrast, in a three-level ladder-system with co-linear probe and control fields, where usually $k_p \neq k_c$, EIT can be greatly enhanced as well as attenuated depending on the ratio k_c/k_p and the relative signs of the wavevectors $\mathbf{k}_c, \mathbf{k}_p$ [48]. This allows the realization of nonreciprocal optics in vapor cells by correct choice of the atomic transitions used for EIT [52].

In this tutorial we discuss the interplay between EIT enhancement and attenuation and wavenumber mismatch in a ladder-type three-level atomic system. We show that for counter-propagating beams a gap appears in the eigenenergy spectrum of the two states dressed by the control field as a function of atomic velocity. Because probe photons cannot be absorbed within this avoided crossing, a box-shaped transmission window inside the Doppler-broadened absorption background opens, which width can be even larger than the EIT window in the case of cold (stationary) atoms under the same control field intensity [48]. We study the dependence of the hot-vapor transmission window width and height on the wavenumber mismatch in detail and determine the optimal relation between k_c and k_p to maximize EIT width. While this ratio is not available for ground-state transitions in the alkali species commonly used in vapor cell EIT experiments [44], it can be achieved in these species in ladder configurations with Rydberg states [15]. We demonstrate the non-reciprocity in an experiment in hot Rubidium vapor, using $|20S\rangle$ as upper state in the ladder-system, and show that the experimental data agrees very well with the theory model.

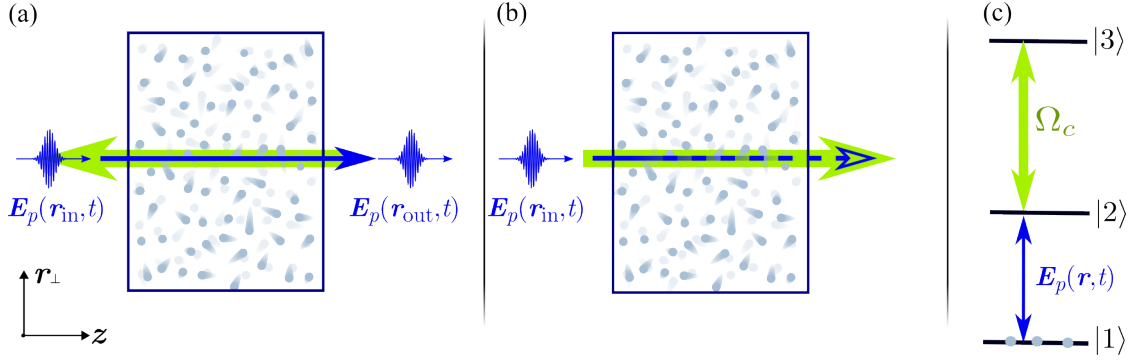


Figure 1. (Color online) The probe $\mathbf{E}_p(\mathbf{r}, t)$ and a classical laser field Ω_c are coupled to a three-level ladder-type hot atomic system shown in (c). When the two fields are counter-propagating, the EIT spectrum for the probe can be recovered in the condition of negative wavenumber mismatch such that the probe photon can fully pass through. When they are co-propagating, the EIT medium is turned into a broadband absorber such that the probe photon is randomly scattering into all directions due to strong absorption.

2. Theoretical model

We consider a three-level ladder atomic system as illustrated in Fig. 1(c). Two successive transitions are coupled by a weak probe Ω_p and a strong control field Ω_c , respectively. In the laboratory frame, the Hamiltonian for the atom-light interaction under the dipole approximation reads

$$\hat{H} = \sum_{j=1}^N \sum_{i=1}^3 \hbar \omega_i \hat{\sigma}_{ii}^{(j)} - (\hat{\mathbf{d}}^{(j)} \cdot \mathbf{E}(\mathbf{r}_j) + H.c.) \quad (1)$$

where $\hbar \omega_i$ is the energy for the state $|i\rangle$, and $\hat{\mathbf{d}}^{(j)}$ is the dipole moment operator of the j -th atom. N is the number of atoms, $H.c.$ stands for Hermitian conjugate. $\mathbf{E}(\mathbf{r}_j)$ denotes the positive-frequency part of the electric field, which we can write as the sum of the two probe and control laser fields, i.e., $\mathbf{E}(\mathbf{r}) = \mathbf{E}_p(\mathbf{r}, t) + \mathbf{E}_c(\mathbf{r}, t) = \mathcal{E}_p(\mathbf{r})e^{i(\mathbf{k}_p \cdot \mathbf{r} - \omega_p t)} + \mathcal{E}_c(\mathbf{r})e^{i(\mathbf{k}_c \cdot \mathbf{r} - \omega_c t)}$. Here \mathbf{k}_p, ω_p and \mathbf{k}_c, ω_c are the wave vectors and frequencies of the probe and control fields, respectively, and $\mathcal{E}_p(\mathbf{r})$ and $\mathcal{E}_c(\mathbf{r})$ denote the slowly-varying amplitude of each field. We further assume that the probe and control laser fields are near-resonant only with the respective atomic transitions, $|1\rangle \leftrightarrow |2\rangle$ and $|1\rangle \leftrightarrow |3\rangle$, such that the Hamiltonian simplifies to

$$\begin{aligned} \hat{H} = & \sum_{j=1}^N \sum_{i=1}^3 \hbar \omega_i \hat{\sigma}_{ii}^{(j)} - [(\mathbf{d}_{21} \hat{\sigma}_{12}^{(j)} + \mathbf{d}_{12} \hat{\sigma}_{21}^{(j)}) \cdot \mathcal{E}_p(\mathbf{r}_j) e^{i(\mathbf{k}_p \cdot \mathbf{r} - \omega_p t)} + H.c.] \\ & - [(\mathbf{d}_{32} \hat{\sigma}_{23}^{(j)} + \mathbf{d}_{23} \hat{\sigma}_{32}^{(j)}) \cdot \mathcal{E}_c(\mathbf{r}_j) e^{i(\mathbf{k}_c \cdot \mathbf{r} - \omega_c t)} + H.c.] \end{aligned} \quad (2)$$

where $\mathbf{d}_{12}^{(j)} = \langle 1_j | \hat{\mathbf{d}}^{(j)} | 2_j \rangle = \mathbf{d}_{12}$ and $\mathbf{d}_{23}^{(j)} = \langle 2_j | \hat{\mathbf{d}}^{(j)} | 3_j \rangle = \mathbf{d}_{23}$ are the dipole moments of the probe and control transition, respectively, and $\hat{\sigma}_{ij}^{(l)} = |i_l\rangle \langle j_l|$ are the corresponding atomic transition operator for the j th atom.

Transforming to a rotating frame via the unitary

$$\hat{U} = \exp \left[i \left(\sum_j \omega_1 t \hat{\sigma}_{11}^{(j)} + (\omega_1 + \omega_p) t \hat{\sigma}_{22}^{(j)} + (\omega_1 + \omega_p + \omega_c) t \hat{\sigma}_{33}^{(j)} \right) \right], \quad (3)$$

and applying the rotating wave approximation, one obtains

$$\frac{H}{\hbar} = - \sum_j (\Delta_p \hat{\sigma}_{22}^{(j)} + (\Delta_p + \Delta_c) \hat{\sigma}_{33}^{(j)}) - \sum_j [\Omega_p(\mathbf{r}_j) e^{i\mathbf{k}_p \cdot \mathbf{r}} \hat{\sigma}_{21}^{(j)} + \Omega_c(\mathbf{r}_j) e^{i\mathbf{k}_c \cdot \mathbf{r}} \hat{\sigma}_{32}^{(j)} + H.c.] \quad (4)$$

where $\Delta_p = \omega_p - (\omega_2 - \omega_1)$ and $\Delta_c = \omega_c - (\omega_3 - \omega_2)$ are the frequency detunings of the probe and control field from their respective atomic transition, and $\Omega_p(\mathbf{r}_j) = \mathbf{d}_{21} \cdot \boldsymbol{\mathcal{E}}_p(\mathbf{r})/\hbar$ and $\Omega_c(\mathbf{r}_j) = \mathbf{d}_{32} \cdot \boldsymbol{\mathcal{E}}_c(\mathbf{r})/\hbar$ denote the Rabi frequencies of the two fields. For simplicity, we will assume that the beam profile of the control-field is significantly broader than that of the probe field, such that one can approximate $\Omega_c(\mathbf{r}_j) = \Omega_c$.

We are interested in the linear probe-field response of the atomic medium. Typically, the beam waist of the probe field is sufficiently large to describe its propagation dynamics by the paraxial wave equation

$$\left[\frac{\partial}{\partial z} - \frac{i}{2k_p} \left(\frac{\partial^2}{\partial x^2} + \frac{\partial^2}{\partial y^2} \right) \right] \boldsymbol{\mathcal{E}}_p(\mathbf{r}) = i \frac{k_p}{\epsilon_0} \mathbf{e}_p^* \cdot \mathbf{P}(\mathbf{r}) e^{-ik_p z} \quad (5)$$

where $\boldsymbol{\mathcal{E}}_p(\mathbf{r}) = \mathbf{e}_p \mathcal{E}_p(\mathbf{r})$ and \mathbf{e}_p is the unit polarization vector. Here, we assume a probe-field propagation along the z -direction, \mathbf{e}_z , such that the probe-field wave vector is $\mathbf{k}_p = k_p \mathbf{e}_z$. $\mathbf{P}(\mathbf{r})$ is the atomic polarization field $\mathbf{P}(\mathbf{r}) = \sum_j \mathbf{d}_{21} \langle \hat{\sigma}_{12}^{(j)} \rangle \delta(\mathbf{r} - \mathbf{r}_j)$, which is given by the atomic coherence $\langle \hat{\sigma}_{12}^{(j)} \rangle$. It is determined by the atomic dynamics that follows from the Heisenberg equations

$$\frac{d\hat{\sigma}}{dt} = \frac{i}{\hbar} [\hat{H}_{\text{int}}, \hat{\sigma}] + \sum_j \frac{\Gamma_2}{2} [2\hat{\sigma}_{12}^{(j)} \hat{\sigma}_{21}^{(j)} - \{\hat{\sigma}_{21}^{(j)} \hat{\sigma}_{12}^{(j)}, \hat{\sigma}\}] + \frac{\Gamma_3}{2} [2\hat{\sigma}_{23}^{(j)} \hat{\sigma}_{32}^{(j)} - \{\hat{\sigma}_{32}^{(j)} \hat{\sigma}_{23}^{(j)}, \hat{\sigma}\}] \quad (6)$$

where Γ_2 and Γ_3 are the spontaneous decay rates of the excited states $|2\rangle$ and $|3\rangle$. Note that one can neglect Langevin noise terms in the above Heisenberg equations, when dealing only with normal ordered operators. The relevant atomic operators therefore evolve as

$$\frac{d\hat{\sigma}_{12}^{(j)}}{dt} = i(\Delta_p + i\frac{\Gamma_2}{2})\hat{\sigma}_{12}^{(j)} + i\Omega_p(\mathbf{r}_j)e^{ik_p z_j}(\hat{\sigma}_{11}^{(j)} - \hat{\sigma}_{22}^{(j)}) + i\Omega_c e^{i\mathbf{k}_c \cdot \mathbf{r}_j} \hat{\sigma}_{13}^{(j)}, \quad (7)$$

$$\frac{d\hat{\sigma}_{13}^{(j)}}{dt} = i(\Delta_p + \Delta_c + i\frac{\Gamma_3}{2})\hat{\sigma}_{13}^{(j)} + i\Omega_c^* e^{-i\mathbf{k}_c \cdot \mathbf{r}_j} \hat{\sigma}_{12}^{(j)}. \quad (8)$$

For $|\Omega_c| \gg |\Omega_p(\mathbf{r})|$, the atoms are only weakly excited, i.e., $\langle \hat{\sigma}_{11}^{(j)} \rangle = 1$ and $\langle \hat{\sigma}_{22}^{(j)} \rangle = 0$. This readily yields the steady state of $\langle \hat{\sigma}_{12}^{(j)} \rangle$ and allows one to reexpress the paraxial wave equation as

$$\left[\frac{\partial}{\partial z} - \frac{i}{2k_p} \left(\frac{\partial^2}{\partial x^2} + \frac{\partial^2}{\partial y^2} \right) \right] \boldsymbol{\mathcal{E}}_p(\mathbf{r}) = i\chi(\Delta_p) \boldsymbol{\mathcal{E}}_p(\mathbf{r}) \quad (9)$$

where the linear susceptibility $\chi(\Delta_p)$ is given by

$$\chi(\Delta_p) = -\frac{3n_0\lambda_p^2\Gamma_2}{8\pi} \frac{1}{\Delta_p + i\frac{\Gamma_2}{2} - \frac{|\Omega_c|^2}{\Delta_p + \Delta_c + i\frac{\Gamma_3}{2}}}. \quad (10)$$

in terms of the atomic density n_0 and the probe-field wavelength $\lambda_p = 2\pi/k_p$. For $\Gamma_3 = 0$ and on two-photon resonance, $\Delta_p + \Delta_c = 0$, the susceptibility $\chi(\Delta_p)$ vanishes, giving rise to EIT susceptibility [7]. Moreover, there are two absorption peaks that are readily understood in a dressed-state picture. To this end we can diagonalize the excited-state Hamiltonian

$$\begin{bmatrix} -\Delta_p & \Omega_c^* e^{-i\mathbf{k}_c \cdot \mathbf{r}} \\ \Omega_c e^{i\mathbf{k}_c \cdot \mathbf{r}} & -\Delta_p - \Delta_c \end{bmatrix} \quad (11)$$

that describes the coupling of $|2\rangle$ and $|3\rangle$ by the control field Ω_c . For $\Delta_c = 0$, the dressed eigenstates are simply $|\pm\rangle = (|2\rangle \pm |3\rangle)/\sqrt{2}$, with corresponding eigenfrequencies $\lambda_{\pm} = \pm|\Omega_c|$. In between the two dressed-state energies, absorption is minimal at two-photon resonance, $\Delta_p + \Delta_c = 0$, and vanishes if $\Gamma_3 = 0$, as mentioned above.

Thermal motion affects the absorption primarily due to the Doppler shift of the atomic transitions. For a given atomic velocity \mathbf{v} , the dressed states are, thus, determined by

$$\begin{bmatrix} -\Delta_p + k_p v_z & \Omega_c^* e^{-i\mathbf{k}_c \cdot \mathbf{r}} \\ \Omega_c e^{i\mathbf{k}_c \cdot \mathbf{r}} & -\Delta_p - \Delta_c + k_p v_z + \mathbf{k}_c \cdot \mathbf{v} \end{bmatrix}, \quad (12)$$

and have eigenfrequencies of

$$\lambda_{\pm} = -\Delta_p + k_p v_z - \frac{1}{2}(\Delta_c - \mathbf{k}_c \cdot \mathbf{v}) \pm \frac{1}{2}\sqrt{(\Delta_c - \mathbf{k}_c \cdot \mathbf{v})^2 + 4|\Omega_c|^2}. \quad (13)$$

The second and third terms in Eq. (13) describe the single-photon Doppler effect on the transition frequency due to the atomic motion, while the last term introduces the frequency shift owing to the combined effect of the control coupling and the Doppler shift. The eigenvalues in Eq. (13) strongly depend on the relative propagation direction of the probe and the control field. Here, we consider two different configurations: (i) counter-propagating fields, such that $\mathbf{k}_c \cdot \mathbf{v} = -k_c v_z$, in terms of the velocity v_z along the z -axis, and (ii) co-propagating fields such that $\mathbf{k}_c \cdot \mathbf{v} = k_c v_z$.

The characteristic velocity-dependence of the dressed-state eigenfrequencies is shown in Fig. 2. For counter-propagating fields and large positive v_z , we have $\lambda_+ \simeq -\Delta_p + k_p v_z$ and $\lambda_- \simeq -\Delta_p - \Delta_c + (k_p - k_c)v_z$. Hence, λ_+ always increases with v_z , while effect of v_z on λ_- depends on the sign of $k_p - k_c$. For $k_c/k_p > 1$ (e.g., $k_c/k_p = 1.5$ or $k_c/k_p = 2.0$), the two states feature an energy gap as a function of v_z [see Fig. 2(a)]. If the frequency of the probe photon lies within this gap, absorption is greatly suppressed and a transparency window can emerge in the velocity-averaged

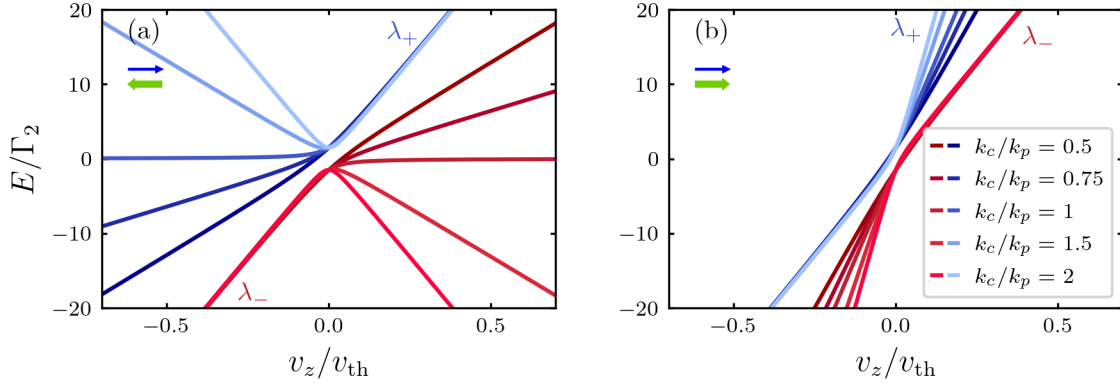


Figure 2. (Color online) Comparison of eigenvalues λ_{\pm} for different ratios k_c/k_p for (a) counter- and (b) co-propagating probe and control fields in a ladder-type EIT scheme. For counter-propagating beams, a frequency gap opens up for $k_c > k_p$, whereas for the counter-propagating fields a frequency gap does not appear. Parameters are $\Delta_c = 0, \Omega_c = 1.5\Gamma_2, \Delta_p = 0$. $\Gamma_2 = 2\pi \times 6.07$ MHz, $\Gamma_3 = 2\pi \times 26.5$ kHz. The temperature is $T = 320$ K.

absorption spectrum. For $k_c/k_p \leq 1$, this avoided crossing disappears and there will be no transparency window in the absorption spectrum.

The eigenvalues for the co-propagating fields [cf. Fig. 1(b)], are shown in Fig. 2(b). In this case, no energy gap exists regardless of k_c/k_p , such that the transparency window is diminished by atomic motion.

The absorption spectrum of a thermal gas is readily obtained from the average

$$\chi(\Delta_p) = -\frac{3n_0\lambda_p^2\Gamma_2}{8\pi} \int_{-\infty}^{\infty} d\mathbf{v} \frac{f_T(\mathbf{v})}{\Delta_p - k_p v_z + i\frac{\Gamma_2}{2} - \frac{|\Omega_c|^2}{\Delta_p + \Delta_c - k_p v_z - \mathbf{k}_c \cdot \mathbf{v} + i\frac{\Gamma_3}{2}}} \quad (14)$$

of the optical susceptibility [see Eq.(10)] over the Maxwell-Boltzmann distribution $f_T(\mathbf{v}) = (\pi v_{th}^2)^{-3/2} e^{-v^2/v_{th}^2}$ of the atomic velocities. Here, $v_{th} = \sqrt{2k_B T/m}$ is the most probable velocity, and T and m are the temperature and mass of the atoms, respectively. The characteristic spectrum of the susceptibility is shown in Fig. 3 for the two field configurations along with the velocity dependence of the dressed-state energies. Indeed, there is a broad transparency window for counter-propagating fields, that can be broader than the EIT window for stationary atoms. Outside of the transparency window there is a broad absorption background due to the Doppler broadening of the probe-field resonance. In stark contrast, one finds flat feature-less absorption background in the co-propagating case. Transparency, thus, emerges from a *negative wavenumber mismatch*, which can not be satisfied for co-propagating fields.

To further illustrate this effect, we calculate the EIT spectrum for different ratios of k_c/k_p for counter-propagating fields. Fig. 4 illustrates the emergence of a transparency window for $k_c/k_p \geq 1$. The width of the transparency window depends on the frequency gap, which is approximately given by

$$\Delta_{\text{EIT}} \simeq \frac{\sqrt{k_p(k_c - k_p)}}{k_c} \cdot 4\Omega_c \quad (15)$$

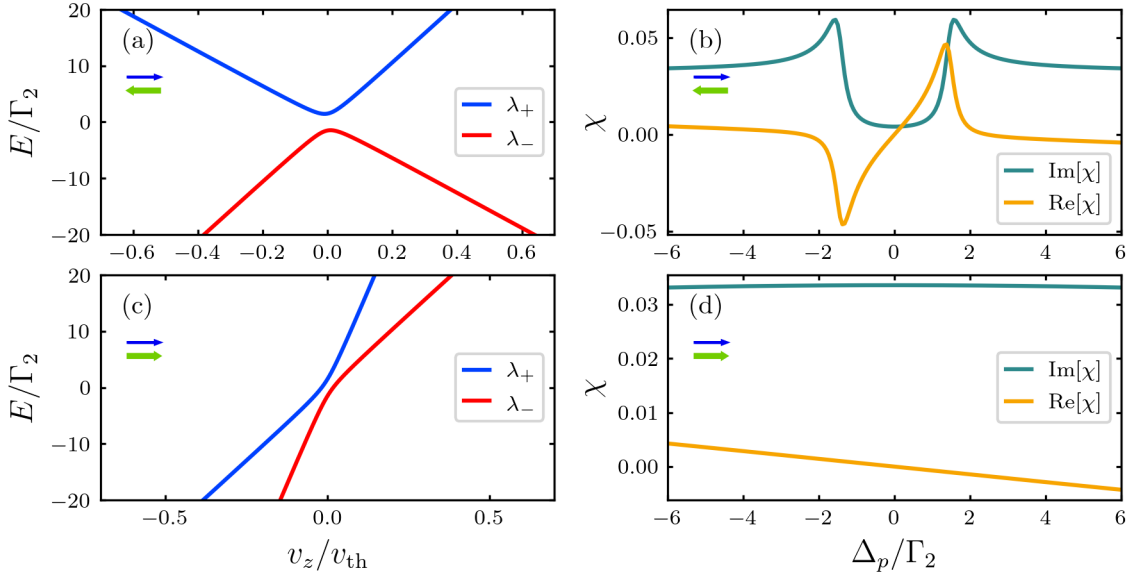


Figure 3. (Color online) (a) The eigenvalues λ_{\pm} as a function of v_z exhibits a frequency gap when the two fields are counter-propagating ($\mathbf{k}_p = k_p \hat{e}_z, \mathbf{k}_c = -k_c \hat{e}_z$), consequently, a box-shaped transparency window is created in the absorption spectrum plotted in (b). (c) The frequency gap is closed when the two fields are co-propagating ($\mathbf{k}_p = -k_p \hat{e}_z, \mathbf{k}_c = -k_c \hat{e}_z$) leading to a Doppler-broadened absorptive spectrum shown in (d). Parameters are $\Delta_c = 0, \Omega_c = 1.5\Gamma_2$. In (a) and (c) we have taken $\Delta_p = 0$. The three states are $5S_{1/2}, 5P_{3/2}$ and $21S_{1/2}$ of ^{87}Rb with transition wavelengths to be $\lambda_p = 780.24 \text{ nm}, \lambda_c = 488.08 \text{ nm}$ and corresponding decay rates $\Gamma_2 = 2\pi \times 6.07 \text{ MHz}, \Gamma_3 = 2\pi \times 26.5 \text{ kHz}$. The temperature is $T = 320 \text{ K}$.

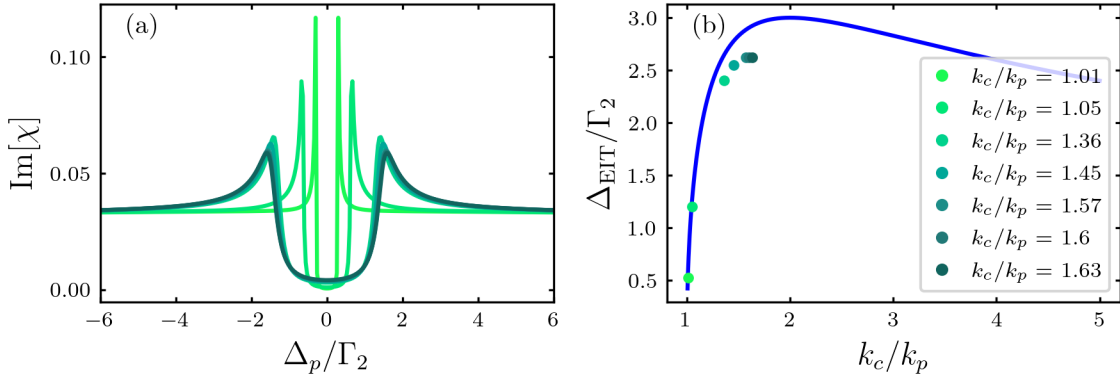


Figure 4. (Color online) (a) The absorption spectrum for different ratio k_c/k_p . Here k_c is changed to show its effect on the transparency window, the ratio k_c/k_p in increasing order corresponds to the case of state 3 chosen to be $5D_{5/2}, 7S_{1/2}, 7D_{5/2}, 10S_{1/2}, 15S_{1/2}, 20S_{1/2}, 100S_{1/2}$ respectively. (b) The solid line shows the approximate width of the EIT window defined by Eq. (15), where the points are obtained from fitting the EIT spectrum plotted in (a). The fitting width is defined as the detuning range in which the absorption is smaller than the background in the two wings. Parameters are the same as in Fig. 3.

for $\Delta_p = \Delta_c = 0$. For $k_c = k_p$ one still observes a narrow EIT window, since in this case the energies of the two dressed states only coincide asymptotically for $v_z \rightarrow \infty$.

Eq. (15) does not account for the finite linewidths of the dressed states, which are given by

$$\Gamma_+ = \Gamma_- = \left[1 - \frac{k_p}{k_c}\right] \Gamma_2 \quad (16)$$

at the state-crossing. When $k_c/k_p \simeq 1$, Γ_{\pm} is very small such that Eq. (15) agrees well with the actual width of the EIT spectrum [see Fig. 4(b)]. For larger values of k_c/k_p , however, the finite linewidth of both states causes deviations from Eq. (15) and slightly reduces the effective width of the EIT window as shown in Fig. 4(b). Nevertheless, the EIT window in hot atoms can be broader than that in cold atoms for a given set of parameters. In this regard, the described negative wavenumber mismatch does not only recover EIT but also improves the transmission of in hot atoms. We finally note that the linear scaling with Ω_c [cf. Eq. (15)] implies that even comparatively weak control fields can generate a significant EIT effect. This is in contrast to a recent experiment on hot atoms [52] in which the generation of transparency required large control-field intensities. This can be understood from the above discussion since the experiment used a state configuration for which $k_c < k_p$ and does therefore not exploit the effect of wavenumber mismatch described above.

3. Experimental demonstration

To demonstrate the EIT recovery with $k_c > k_p$ we perform a proof of principle experiment in a room-temperature vapor of Rb atoms. The setup is shown in Fig. 5 (b) along with the level scheme of the transitions used for the probe and control light in Fig. 5 (b). The experiments are performed in a glass cell with length $L = 5$ cm that contains the isotopes ^{85}Rb and ^{87}Rb at their natural abundance and at $T \approx 296$ K.

The probe light with wavelength $\lambda_p = 780$ nm couples the ground state $|1\rangle = |5S_{1/2}, F = 2\rangle$ to a hyperfine manifold of intermediate states $|2\rangle = |5P_{3/2}, F = 1, 2, 3\rangle$ in ^{87}Rb and $|1\rangle = |5S_{1/2}, F = 3\rangle$ to $|2\rangle = |5P_{3/2}, F = 2, 3, 4\rangle$ in ^{85}Rb . We focus the probe light to a waist of ≈ 50 μm . The control light with wavelength $\lambda_c = 488$ nm and intensity 0.66 W couples $|2\rangle$ to a low-lying Rydberg state $|3\rangle = |20S_{1/2}\rangle$ and is focused to a waist of ≈ 70 μm .

The peak Rabi frequency in the focus is $\approx 19\Gamma$, while the effective Rabi frequency across the entire length of the vapor cell is significantly lower. The discrepancy in wavelength leads to $k_c/k_p = \lambda_p/\lambda_c \approx 1.6$. Fig. 4 shows that one expects an EIT window with significant width for this ratio.

To investigate both co- and counter-propagating probe and control fields, the setup is build symmetrically, such that the probe light can be sent through the glass cell from both sides. After the cell, the probe light is coupled into a single-mode fiber and detected on a single-photon counter. This signal can be compared to a reference signal picked up before the glass cell and detected on a different single-photon counter.

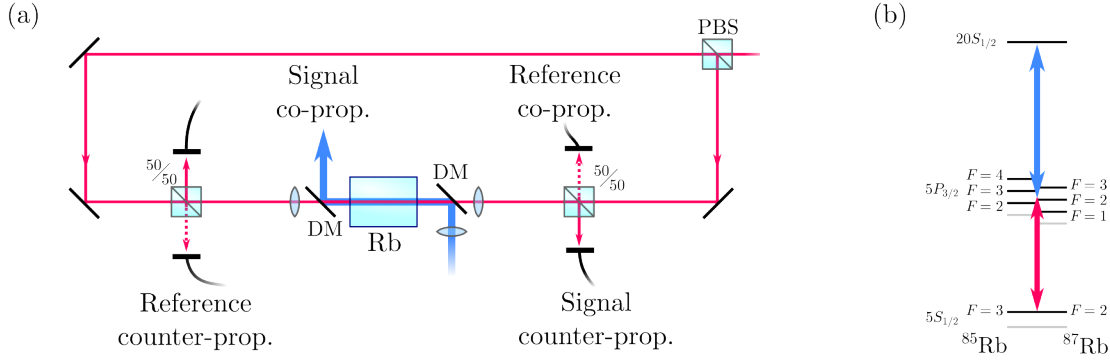


Figure 5. (Color online) Schematics of experimental setup for measuring hot EIT with probe and control beams in co- and counter-propagating configuration. The probe beams for the two configurations are split from the same incoming beam and passed through the setup in opposite direction. Before the vapor cell, each beam is split on a beam splitter to obtain a reference signal without atoms. The transmission signal through the vapor cell and the reference signal are fiber coupled and measured on single-photon counter modules. The resulting transmissions are shown in Fig. 6. The control beam is overlapped with the probe beam on two dichroic mirrors (DM).

Fig. 6 (a) and (b) show the transmission of a weak probe beam with peak intensity a factor of > 100 below saturation as we scan the probe detuning Δ_p over the Doppler-broadened probe transitions for both isotopes. For counter-propagating probe and control light, we observe multiple EIT resonances that arise from the different hyperfine levels of the intermediate state $|2\rangle$. In the case of copropagating probe and control, the EIT resonances are absent as predicted by theory. Comparing the experimental data to theory, we find excellent agreement of the respective transmission curves for $\Delta_c = 13\Gamma_2$, $\Omega_c = 7\Gamma_2$.

Besides spontaneous decay from the intermediate state $|2\rangle$ with rate Γ_2 , we have also phenomenologically introduced additional decay from $|2\rangle$ with rates $\gamma_{87} = 5\Gamma_2$ (for ^{87}Rb) and $\gamma_{85} = 3\Gamma_2$ (^{85}Rb). This additional decay would include the diffraction of the probe beam which causes absorption when its size is larger than the control beam, imperfect polarization of the laser beams, collisional broadening and other experimental imperfections [53, 54].

4. Summary and outlook

In this tutorial we have presented a theoretical analysis of a Doppler-broadened three-level ladder-system and pointed out that while atomic motion limits the visibility of EIT for certain positive wavenumber mismatch, EIT is recovered and enhanced for negative wavenumber mismatch where the control field has a wavenumber larger than that of the probe field.

We have demonstrated this effect in an experiment with hot Rubidium atoms where a Rydberg state is used to obtain a wavevector ratio so that $k_p < k_c$ is satisfied for counter-propagating probe and control fields. In the experiment, the width of the EIT

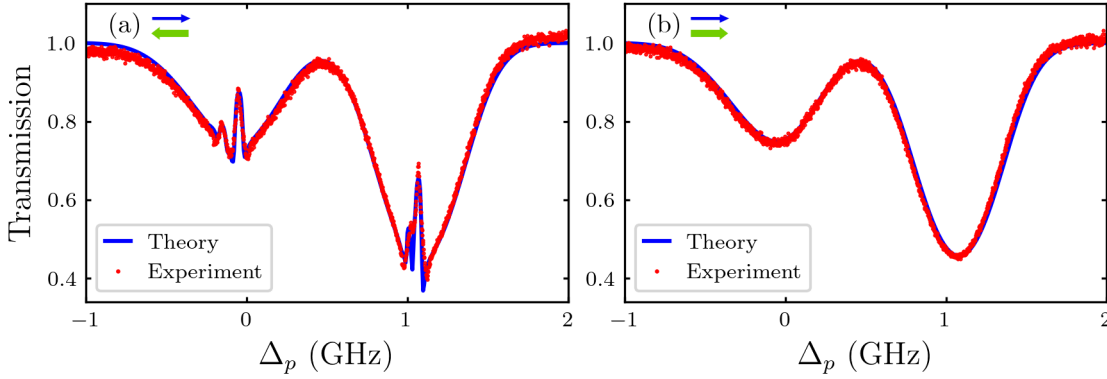


Figure 6. (Color online) Experimental observation of direction-dependent recovery of EIT in a Rb vapor for counter- (a) and co-propagating (b) probe and control beams. Besides the experimental data (red) we also show the theoretically predicted transmission (blue) for $\Delta_c = 13\Gamma_2$, $\Omega_c = 7\Gamma_2$ and additional phenomenological decay from the intermediate state with rates $\gamma_{87} = 5\Gamma_2$ and $\gamma_{85} = 3\Gamma_2$ for ^{87}Rb and ^{85}Rb respectively. All other parameters are the same as in Fig. 3.

window is limited by available control beam power, but the calculations show that it scales favorably with the wavelength mismatch in hot atomic vapors and can even exceed what can be reached without Doppler broadening for the same laser powers.

The mechanism discussed here is not limited to the three-level ladder-system. Similar conditions on the wavenumber mismatch exists for lambda systems [48], and the theory may be further extended to systems with more levels and coupling lasers to employ negative three-photon or even high-order wavenumber mismatch [55, 56]. A direct application of the non-reciprocal transmission in the three-level system is the realization of magnetic field-free high-fidelity optical isolators [52, 57–59]. The relative simplicity of the scheme lends itself to combination with nano-optical structures or miniaturized vapor cells to realize on-chip optical isolators and circulators [60–67]. Finally, as for alkali atoms $k_c > k_p$ is satisfied when a ladder-system with a Rydberg state is used, this opens the opportunity of combining enhanced EIT with Rydberg-mediated photon-photon interaction for realization of nonlinear quantum optics [28, 68–71].

All of these points serve to highlight how the Doppler effect in hot atomic vapors, which is often seen as a hindrance, can be utilized in EIT systems to realize nonreciprocal optics in hot atoms with wide-ranging applications.

Acknowledgements

This work was supported by the European Union through the Horizon 2020 program under the ERC consolidator grant RYD-QNLO (grant no. 771417) and through the Horizon Europe ERC synergy grant SuperWave (grant no. 101071882). The work was also supported by the Carlsberg Foundation through the Semper Ardens Research Project QCool.

Data availability

The experimental data for Fig. 6, and the code for creating all figures in this tutorial are available in the Zenodo database under accession code <https://doi.org/10.5281/zenodo.10689011>

References

- [1] Harris S E, Field J E and Imamoglu A 1990 *Phys. Rev. Lett.* **64**(10) 1107–1110 URL <https://link.aps.org/doi/10.1103/PhysRevLett.64.1107>
- [2] Boller K J, Imamoglu A and Harris S E 1991 *Phys. Rev. Lett.* **66**(20) 2593–2596 URL <https://link.aps.org/doi/10.1103/PhysRevLett.66.2593>
- [3] Fleischhauer M and Lukin M D 2000 *Phys. Rev. Lett.* **84**(22) 5094–5097 URL <https://link.aps.org/doi/10.1103/PhysRevLett.84.5094>
- [4] Fleischhauer M and Lukin M D 2002 *Phys. Rev. A* **65**(2) 022314 URL <https://link.aps.org/doi/10.1103/PhysRevA.65.022314>
- [5] Liu C, Dutton Z, Behroozi C H and Hau L V 2001 *Nature* **409** 490–493 ISSN 1476-4687 URL <https://doi.org/10.1038/35054017>
- [6] Phillips D F, Fleischhauer A, Mair A, Walsworth R L and Lukin M D 2001 *Phys. Rev. Lett.* **86**(5) 783–786 URL <https://link.aps.org/doi/10.1103/PhysRevLett.86.783>
- [7] Fleischhauer M, Imamoglu A and Marangos J P 2005 *Rev. Mod. Phys.* **77**(2) 633–673 URL <https://link.aps.org/doi/10.1103/RevModPhys.77.633>
- [8] Gorshkov A V, André A, Lukin M D and Sørensen A S 2007 *Phys. Rev. A* **76**(3) 033805 URL <https://link.aps.org/doi/10.1103/PhysRevA.76.033805>
- [9] van der Wal C H, Eisaman M D, André A, Walsworth R L, Phillips D F, Zibrov A S and Lukin M D 2003 *Science* **301** 196–200 ISSN 1095-9203
- [10] Maxwell D, Szwer D J, Paredes-Barato D, Busche H, Pritchard J D, Gauguet A, Weatherill K J, Jones M P A and Adams C S 2013 *Physical Review Letters* **110** 103001 ISSN 1079-7114
- [11] Dudin Y O, Li L and Kuzmich A 2013 *Physical Review A* **87** 031801 ISSN 1094-1622
- [12] Lampen J, Nguyen H, Li L, Berman P R and Kuzmich A 2018 *Physical Review A* **98** 033411 ISSN 2469-9934
- [13] Katz O and Firstenberg O 2018 *Nature Communications* **9** ISSN 2041-1723
- [14] Buser G, Mottola R, Cotting B, Wolters J and Treutlein P 2022 *PRX Quantum* **3** 020349 ISSN 2691-3399
- [15] Mohapatra A K, Jackson T R and Adams C S 2007 *Phys. Rev. Lett.* **98**(11) 113003 URL <https://link.aps.org/doi/10.1103/PhysRevLett.98.113003>
- [16] Mohapatra A K, Bason M G, Butscher B, Weatherill K J and Adams C S 2008 *Nature Physics* **4** 890–894 ISSN 1745-2481
- [17] Sedlacek J A, Schwettmann A, Kübler H, Löw R, Pfau T and Shaffer J P 2012 *Nature Physics* **8** 819–824
- [18] Sedlacek J A, Schwettmann A, Kübler H and Shaffer J P 2013 *Phys. Rev. Lett.* **111**(6) 063001 URL <http://link.aps.org/doi/10.1103/PhysRevLett.111.063001>
- [19] Ma L, Anderson D A and Raithel G 2017 *Physical Review A* **95** 061804 ISSN 2469-9934
- [20] Downes L A, MacKellar A R, Whiting D J, Bourgenot C, Adams C S and Weatherill K J 2020 *Physical Review X* **10** 011027 ISSN 2160-3308
- [21] Meyer D H, Kunz P D and Cox K C 2021 *Phys. Rev. Applied* **15**(1) 014053 URL <https://link.aps.org/doi/10.1103/PhysRevApplied.15.014053>
- [22] Zhang L H, Liu Z K, Liu B, Zhang Z Y, Guo G C, Ding D S and Shi B S 2022 *Phys. Rev. Applied* **18**(1) 014033 URL <https://link.aps.org/doi/10.1103/PhysRevApplied.18.014033>
- [23] Pritchard J D, Maxwell D, Gauguet A, Weatherill K J, Jones M P A and Adams C S 2010

- Phys. Rev. Lett.* **105**(19) 193603 URL <https://link.aps.org/doi/10.1103/PhysRevLett.105.193603>
- [24] Saffman M, Walker T G and Mølmer K 2010 *Rev. Mod. Phys.* **82**(3) 2313–2363 URL <https://link.aps.org/doi/10.1103/RevModPhys.82.2313>
- [25] Gorshkov A V, Otterbach J, Fleischhauer M, Pohl T and Lukin M D 2011 *Phys. Rev. Lett.* **107**(13) 133602 URL <https://link.aps.org/doi/10.1103/PhysRevLett.107.133602>
- [26] Peyronel T, Firstenberg O, Liang Q Y, Hofferberth S, Gorshkov A V, Pohl T, Lukin M D and Vuletić V 2012 *Nature* **488** 57–60 ISSN 1476-4687 URL <https://doi.org/10.1038/nature11361>
- [27] Dudin Y O and Kuzmich A 2012 *Science* **336** 887–889 URL <https://www.science.org/doi/abs/10.1126/science.1217901>
- [28] Ripka F, Kübler H, Löw R and Pfau T 2018 *Science* **362** 446–449 URL <https://www.science.org/doi/abs/10.1126/science.aau1949>
- [29] Finkelstein R, Poem E, Michel O, Lahad O and Firstenberg O 2018 *Science Advances* **4** ISSN 2375-2548
- [30] Dideriksen K B, Schmiege R, Zugenmaier M and Polzik E S 2021 *Nature Communications* **12** ISSN 2041-1723
- [31] Li L, Dudin Y O and Kuzmich A 2013 *Nature* **498** 466–469 URL <http://www.nature.com/nature/journal/v498/n7455/full/nature12227.html>
- [32] Baur S, Tiarks D, Rempe G and Dürr S 2014 *Phys. Rev. Lett.* **112**(7) 073901 URL <https://link.aps.org/doi/10.1103/PhysRevLett.112.073901>
- [33] Tiarks D, Baur S, Schneider K, Dürr S and Rempe G 2014 *Phys. Rev. Lett.* **113**(5) 053602 URL <https://link.aps.org/doi/10.1103/PhysRevLett.113.053602>
- [34] Gorniaczyk H, Tresp C, Schmidt J, Fedder H and Hofferberth S 2014 *Phys. Rev. Lett.* **113**(5) 053601 URL <https://link.aps.org/doi/10.1103/PhysRevLett.113.053601>
- [35] Tresp C, Zimmer C, Mirgorodskiy I, Gorniaczyk H, Paris-Mandoki A and Hofferberth S 2016 *Phys. Rev. Lett.* **117**(22) 223001 URL <https://link.aps.org/doi/10.1103/PhysRevLett.117.223001>
- [36] Stiesdal N, Busche H, Kleinbeck K, Kumlin J, G Hansen M, Büchler H P and Hofferberth S 2021 *Nature Communications* **12** 4328 ISSN 2041-1723 URL <https://doi.org/10.1038/s41467-021-24522-w>
- [37] Tiarks D, Schmidt S, Rempe G and Dürr S 2016 *Science Advances* **2** e1600036 URL <https://www.science.org/doi/abs/10.1126/sciadv.1600036>
- [38] Murray C R and Pohl T 2017 *Phys. Rev. X* **7**(3) 031007 URL <https://link.aps.org/doi/10.1103/PhysRevX.7.031007>
- [39] Tiarks D, Schmidt-Eberle S, Stolz T, Rempe G and Dürr S 2019 *Nature Physics* **15** 124–126 ISSN 1745-2481 URL <https://doi.org/10.1038/s41567-018-0313-7>
- [40] Gea-Banacloche J, Li Y q, Jin S z and Xiao M 1995 *Phys. Rev. A* **51**(1) 576–584 URL <https://link.aps.org/doi/10.1103/PhysRevA.51.576>
- [41] Xiao M, Li Y q, Jin S z and Gea-Banacloche J 1995 *Phys. Rev. Lett.* **74**(5) 666–669 URL <https://link.aps.org/doi/10.1103/PhysRevLett.74.666>
- [42] Shepherd S, Fulton D J and Dunn M H 1996 *Phys. Rev. A* **54**(6) 5394–5399 URL <https://link.aps.org/doi/10.1103/PhysRevA.54.5394>
- [43] Vemuri G and Agarwal G S 1996 *Physical Review A* **53** 1060–1064 ISSN 1094-1622
- [44] Badger S D, Hughes I G and Adams C S 2001 *Journal of Physics B: Atomic, Molecular and Optical Physics* **34** L749–L756 ISSN 1361-6455
- [45] Noh H R and Moon H S 2012 *Journal of Physics B: Atomic, Molecular and Optical Physics* **45** 245002 ISSN 1361-6455 URL <https://iopscience.iop.org/article/10.1088/0953-4075/45/24/245002>
- [46] Urvoy A, Carr C, Ritter R, Adams C S, Weatherill K J and Löw R 2013 *Journal of Physics B: Atomic, Molecular and Optical Physics* **46** 245001 ISSN 1361-6455 URL <https://iopscience.iop.org/article/10.1088/0953-4075/46/24/245001>

- iop.org/article/10.1088/0953-4075/46/24/245001
- [47] Fulton D J, Shepherd S, Moseley R R, Sinclair B D and Dunn M H 1995 *Phys. Rev. A* **52**(3) 2302–2311 URL <https://link.aps.org/doi/10.1103/PhysRevA.52.2302>
- [48] Boon J R, Zekou E, McGloin D and Dunn M H 1999 *Physical Review A* **59** 4675–4684 ISSN 1094-1622
- [49] Li Y q and Xiao M 1995 *Physical Review A* **51** R2703–R2706 ISSN 1094-1622
- [50] Carvalho P R S, de Araujo L E E and Tabosa J W R 2004 *Phys. Rev. A* **70**(6) 063818 URL <https://link.aps.org/doi/10.1103/PhysRevA.70.063818>
- [51] Novikova I, Walsworth R and Xiao Y 2012 *Laser & Photonics Reviews* **6** 333–353 URL <https://onlinelibrary.wiley.com/doi/abs/10.1002/lpor.201100021>
- [52] Dong M X, Xia K Y, Zhang W H, Yu Y C, Ye Y H, Li E Z, Zeng L, Ding D S, Shi B S, Guo G C and Nori F 2021 *Science Advances* **7** eabe8924 URL <https://www.science.org/doi/abs/10.1126/sciadv.abe8924>
- [53] Kumar M A and Singh S 2009 *Physical Review A* **79** 063821 ISSN 1094-1622
- [54] Finkelstein R, Bali S, Firstenberg O and Novikova I 2023 *New Journal of Physics* **25** 035001 ISSN 1367-2630
- [55] Mirza A B and Singh S 2012 *Physical Review A* **85** 053837 ISSN 1094-1622
- [56] Thaicharoen N, Moore K R, Anderson D A, Powel R C, Peterson E and Raithel G 2019 *Physical Review A* **100** 063427 ISSN 2469-9934
- [57] Xia K, Nori F and Xiao M 2018 *Phys. Rev. Lett.* **121**(20) 203602 URL <https://link.aps.org/doi/10.1103/PhysRevLett.121.203602>
- [58] Hao Y M, Lin G W, Lin X M, Niu Y P and Gong S Q 2019 *Scientific Reports* **9** 4723 ISSN 2045-2322 URL <https://doi.org/10.1038/s41598-019-41185-2>
- [59] Li E Z, Ding D S, Yu Y C, Dong M X, Zeng L, Zhang W H, Ye Y H, Wu H Z, Zhu Z H, Gao W, Guo G C and Shi B S 2020 *Phys. Rev. Res.* **2**(3) 033517 URL <https://link.aps.org/doi/10.1103/PhysRevResearch.2.033517>
- [60] Ghosh S, Sharping J E, Ouzounov D G and Gaeta A L 2005 *Physical Review Letters* **94** 093902 ISSN 1079-7114
- [61] Benabid F, Light P S, Couny F and Russell P S 2005 *Optics Express* **13** 5694 ISSN 1094-4087
- [62] Kübler H, Shaffer J P, Baluktsian T, Löw R and Pfau T 2010 *Nature Photonics* **4** 112–116 ISSN 1749-4893
- [63] Keaveney J, Sargsyan A, Krohn U, Hughes I G, Sarkisyan D and Adams C S 2012 *Phys. Rev. Lett.* **108**(17) 173601 URL <http://link.aps.org/doi/10.1103/PhysRevLett.108.173601>
- [64] Sayrin C, Junge C, Mitsch R, Albrecht B, O’Shea D, Schneeweiss P, Volz J and Rauschenbeutel A 2015 *Phys. Rev. X* **5**(4) 041036 URL <http://link.aps.org/doi/10.1103/PhysRevX.5.041036>
- [65] Scheucher M, Hilico A, Will E, Volz J and Rauschenbeutel A 2016 *Science* **354** 1577–1580 URL <https://doi.org/10.1126/science.aaj2118>
- [66] Zektzer R, Mazurski N, Barash Y and Levy U 2021 *Nature Photonics* **15** 772–779 ISSN 1749-4893 URL <https://doi.org/10.1038/s41566-021-00853-4>
- [67] Mottola R, Buser G and Treutlein P 2023 *Physical Review Letters* **131** 260801 ISSN 1079-7114 URL <https://doi.org/10.1103/PhysRevLett.131.260801>
- [68] Pritchard J, Weatherill K and Adams C 2013 *Annual review of cold atoms and molecules* **1** 301–350
- [69] Chang D E, Vuletic V and Lukin M D 2014 *Nature Photonics* **8** 685–694 URL <https://www.nature.com/articles/nphoton.2014.192>
- [70] Murray C and Pohl T 2016 Chapter seven - quantum and nonlinear optics in strongly interacting atomic ensembles (*Advances In Atomic, Molecular, and Optical Physics* vol 65) ed Arimondo E, Lin C C and Yelin S F (Academic Press) pp 321 – 372 URL <http://www.sciencedirect.com/science/article/pii/S1049250X1630009X>
- [71] Firstenberg O, Adams C S and Hofferberth S 2016 *Journal of Physics B: Atomic, Molecular and Optical Physics* **49** 152003 URL <http://stacks.iop.org/0953-4075/49/i=15/a=152003>